H1-Integrity of Carrier Phase Navigation Algorithms Using Multiple Reference Receivers

Samer Khanafseh, Steven Langel and Boris Pervan
Illinois Institute of Technology, Chicago, IL

ABSTRACT

In this paper, a methodology is developed to evaluate carrier phase navigation architectures under reference receiver failure. Different approaches to utilize redundant carrier phase measurements from multiple reference receivers are described. Carrier phase measurements are used to provide high accuracy estimates of a user's position. But in precision approach applications that involve safety-of-life, such as in autonomous shipboard landing, integrity also plays a critical role. One case where the system integrity becomes at risk is in the situation of GPS reference receiver failure. Integrity risk in these applications is kept at a minimum by equipping the ship (reference station) with redundant receivers. In this paper, we investigate the impact of different methods on accuracy and integrity from several perspectives, including availability performance, cycle resolution capabilities, implementation complexity and computational efficiency.

I. INTRODUCTION

Carrier phase measurements can be used to provide high accuracy estimates of a user's position. For life-critical GNSS applications, such as civil aircraft approach with a Ground Based Augmentation System (GBAS), extremely high levels of integrity are required. For example, for a Category I system, integrity risk on the order of 10^{-7} per aircraft approach is needed with a vertical position alert limit of 10 m. However, the accuracy requirements for the GBAS application (vertical 95% accuracy on the order of 2 m) are not stringent enough to require the use of high precision carrier phase navigation [1]. As a result, these applications are usually based on punctual (snapshot) positioning using carrier-smoothed code. This situation is in direct contrast to the autonomous shipboard landing application in which the highly dynamic nature of the aircraft and the ship, as well as the need for complete autonomy, requires high levels of integrity and accuracy simultaneously. Therefore, in order to achieve centimeter-level positioning accuracy using carrier phase measurements, the resolution of cycle ambiguities is necessary.

The integrity of the navigation system is at risk when the reference receiver fails. This scenario is usually avoided by equipping the reference station (ship) with multiple receivers, which provide redundancy for estimation and a means for reference receiver failure mitigation. Although multiple reference receivers are usually used for integrity, it is possible to utilize these redundant measurements to enhance accuracy as well. The improvement in accuracy that is achievable depends heavily on how these measurements are combined. In this work we provide two different approaches to process the redundant measurements from the reference receivers (ship-based in the shipboard landing case). The first method is a position domain weighted average position solution, where each track estimates a position and then the individual solutions are averaged to provide one solution. The second one is referred to as the range domain coupled estimation approach. In this method, the measurements from all reference receivers are coupled with airborne measurements in the range domain and used to estimate a unified solution.

Although multiple reference receivers can be used to improve the system accuracy, the main purpose for installing multiple reference receivers in the reference station is for integrity. Therefore, the integrity risk of the navigation system must comply with the integrity requirement under the fault-free hypothesis (H0), the single-receiver-failure hypothesis (H1) and all other failure hypotheses. H0 and H1 hypotheses are the main focus of this paper and therefore all other failure hypotheses (multi-receiver failures, signal in space failures, etc.) will not be discussed. Although the literature provides solutions for the integrity under the H1 hypothesis for snapshot navigation systems (such as GBAS) [1-3], H1 integrity for carrier phase navigation

algorithms has not been discussed previously. As we will show in this paper, the necessity of estimating and resolving the cycle ambiguities is the main challenge in evaluating H1 integrity for high accuracy carrier phase navigation applications.

In this paper, we will start by developing a methodology to mitigate single-receiver failure and meet H1 integrity requirements for carrier phase navigation architectures. Next, different approaches to the processing of measurements from redundant receivers are described. Finally, we investigate the impact of these approaches on accuracy and integrity (both H0 and H1) from different perspectives including availability performance, cycle resolution capabilities, complexity and computational efficiency.

II. H1 HYPOTHESIS MITIGATION ALGORITHM

The H1 Hypothesis is defined as a fault associated with any one, and only one, reference receiver. A fault includes any anomalous measurement that is not immediately detected by the reference station. Therefore, the broadcast data are affected, which induces errors in the airborne system. In this work, the shipboard-landing reference receiver mitigation algorithm will be based on the LAAS H1 algorithm. However because of the differences between the navigation algorithms in the two systems, significant modifications are necessary.

The LAAS navigation algorithm is a punctual estimation system that uses smoothed pseudorange measurements and estimates the user position with respect to the reference receivers by least squares estimation process [1]. Because of the mobility of the reference station in the shipboard landing application, higher levels of accuracy are required than for similar precision approach applications at land-based airfields (LAAS for example). In addition, to ensure safety and operational usefulness, the navigation architecture must provide high levels of integrity and availability. Because of the highly stringent requirements, the navigation system is based on carrier phase differential GPS (CPDGPS) positioning. In order to benefit from the high precision of CPDGPS, the correct resolution of cycles must be ensured. A number of methods have been used in prior work to aid in the cycle resolution. For example, satellite motion can provide the observability of the cycle ambiguities [7]. Unfortunately the rate of satellite motion is relatively slow in comparison with the time scales of aviation applications such as precision approach and landing.

Heo, et al. have proposed a GPS navigation algorithm for autonomous shipboard landing applications where geometry free/divergence free code-carrier filtering is performed continuously for visible satellites on both the aircraft and the ship until the aircraft is close to the ship [8, 9]. Geometry-free observable [10], by definition, does not depend on the geometry of the satellites or the user location and eliminates all error sources except for receiver noise and multipath. A geometry free measurement of the widelane cycle ambiguity is formed by subtracting the narrowlane pseudorange from the widelane carrier [7, 10]. A drawback of the geometry free measurement is the presence of higher noise relative to the L1 and L2 carrier phase measurements. This can be overcome by filtering the geometry free measurement over time prior to the final approach. In order to model colored multipath noise in the geometry free measurements, a first order Gauss-Markov measurement error model is used. The outputs of the filtering process are the floating widelane cycle ambiguity estimates. When the aircraft is close to the ship, L1/L2 cycle ambiguity estimates can be extracted with the aid of the satellite geometric redundancy [8, 11]. Next, the cycle ambiguities are fixed using the bootstrap method [12]. The bootstrap rounding process is performed for those ambiguities that can be fixed with a probability of incorrect fix (PIF) that is compliant with the integrity risk requirement. The remaining ambiguities remain floating. The details of the navigation algorithms are outside the scope of this paper but can be found in [4, 5, 9]. All these differences between LAAS and the shipboard landing navigation algorithm present tremendous challenges in H1 mitigation for the navigation algorithm, as we will see in this paper.

Although the reference station (ship) might be the intuitive place to design a monitor to detect receiver failures, many obstacles exist in this scheme. For example, the ship has no access to air measurements including the number of visible satellites, geometries, how long the airborne system has been filtering widelane observables, how long ambiguities have been filtered and how many ambiguities have been fixed. Therefore, in the current algorithm, it is quite hard for a ship monitor to predict the effect of an undetected reference receiver on the aircraft position estimate. Although such a monitor might be useful in maintaining a low probability of multi-receiver failure, it is insufficient for H1 integrity. As a result, the H1 hypothesis must be mitigated in the airborne architecture. The prior probability of H1-hypothesis event is referred to as $P(H_1) = 1\times10^{-5}$ [1].

In fault detection algorithms, it is a common practice to compute a test statistic and compare it to a predefined threshold in order to detect failures. In receiver failure detection, as we will see shortly, the vertical protection level under the H1 hypothesis (VPL_{H1}) and the vertical alert limit (VAL) represent the test statistics and the threshold, respectively. If the reference station is equipped with M number of receivers, it is possible that any one of these receivers will fail. Therefore, under the

hypothesis of a failure in the j^{th} receiver, a corresponding value of VPL_{H1j} is computed. In order to be conservative, VPL_{H1} is defined as the maximum value of all VPL_{H1j}.

$$VPL_{H1} = \max_{j=1:M} \left\{ VPL_{H1j} \right\} \tag{1}$$

However, at any instant, we do not know which hypothesis is true, H0 or H1. Therefore, the maximum value of VPL_{H0} and VPL_{H1} will be the resultant vertical protection level VPL that is compared to VAL.

$$VPL = \max\left\{ VPL_{H0}, VPL_{H1} \right\} \tag{2}$$

Before calculating VPL, the probability of vertical misleading information $P_v(MI)$ needs to be determined from the integrity tree budget. In this work, the probability of misleading information $P_v(MI)$ is defined as the probability of vertical misleading information due to H0 and H1 hypotheses only. H2 hypothesis (events not covered by H0 or H1 such as ranging source faults and simultaneous multiple reference receiver faults) are allocated a separate budget from the total integrity risk. Since the H0 and H1 hypotheses are mutually exclusive and exhaustive events, $P_v(MI)$ can be written as,

$$\begin{aligned} P_v(MI) &= P_v(MI \mid H_0)\ P(H_0) \\ &\quad + \sum_{j=1}^{M} P_v(MI \mid H_{1j})\ P(H_{1j}) \end{aligned} \tag{3}$$

where,

$$P(H_{1j}) = P(H_1) \big/ M$$
$$P(H_0) = 1 - M\,P(H_1) - P(other) \approx 1$$

In this work we assume a static equal allocation of $P_v(MI)$ for all H0 and H1j hypotheses. Therefore, each hypothesis will have an equal integrity risk budget of $P_v(MI)/(M+1)$. As a result, $P_v(MI \mid H_0)$ and $P_v(MI \mid H_{1j})$ become,

$$P_v(MI \mid H_0) = \frac{P_v(MI)}{(M+1)\,P(H_0)} \cong \frac{P_v(MI)}{(M+1)} \tag{4}$$

$$\begin{aligned} P_v(MI \mid H_{1j}) &= \frac{P_v(MI)}{(M+1)\left(P(H_1) \big/ M \right)} \\ &= \frac{M\,P_v(MI)}{(M+1)P(H_1)} \end{aligned} \tag{5}$$

From $P_v(MI|H_0)$, a probability coefficient or 'K value' (referred to as K_{ffmd}) is computed which is used to establish VPL_{H0} as,

$$VPL_{H0} = K_{ffmd}\,\sigma_{v|H0} \tag{6}$$

where $\sigma_{v|H0}$ is the standard deviation of the vertical estimate error under the H0 hypothesis (all reference receivers have been used).

From $P(MI|H_{1j})$, another K value (referred to as K_{md}) is computed which is used to establish VPL_{H1j}. However, VPL_{H1j} represents a faulty scenario which is supposed to induce errors (biases) in the position solution. For VPL_{H1j}, the best estimate of the failure magnitude (bias) is the difference between the vertical estimate based on the H0 and H1j hypotheses $|v_0 - v_{1j}|$. Therefore, VPL_{H1j} is computed as,

$$VPL_{H1j} = \left| v_0 - v_{1j} \right| + K_{md}\,\sigma_{v|H1j} \tag{7}$$

where $\sigma_{v|H1j}$ is the standard deviation of the vertical estimate error under the H1j hypothesis (using all reference receivers except the j^{th} receiver). Notice that, in order to compute VPL_{H1j}, it is necessary to have access to the relative position estimates (v_0 and v_{1j}), which are necessary to compute $|v_0 - v_{1j}|$. Therefore, the calculation of VPL_{H1j} requires access to the measurements and needs to be executed epoch by epoch.

Since both v_0 and v_{1j} are estimated subject to measurement noise, they are both random time sequences. Therefore, the term $|v_0 - v_{1j}|$ in Equation 7 is random, which makes VPL_{H1j} random as well. The randomness in VPL_{H1j} might cause VPL to exceed VAL even though the j^{th} receiver is fault free. This in turn will trigger a false alarm. The probability of false alarm due to the randomness in $|v_0 - v_{1j}|$ must comply with the corresponding fault free continuity risk requirement. In response, a predictive VPL_{H1j} (referred to as $PVPL_{H1j}$) is computed taking into account the randomness of $|v_0 - v_{1j}|$ through $\sigma_{|v0\text{-}v1j|}$ and a K value (referred to as K_{ffc}) that is based on the fault free continuity risk requirement as in Equation 8.

$$PVPL_{H1j} = K_{ffc}\,\sigma_{|v_0 - v_{1j}|} + K_{md}\,\sigma_{v|H1j} \tag{8}$$

Before initiating the approach, $PVPL_{H1j}$ is computed for the whole approach. If $PVPL_{H1j}$ exceeds VAL, then the probability of VPL_{H1j} exceeding VAL due to the randomness in $|v_0 - v_{1j}|$ exceeds the continuity risk requirement. In other words, the predicted continuity risk for the approach exceeds the continuity risk required by the navigation architecture and the approach must not be initiated.

Although computing VPL_{H0} and VPL_{H1j} was addressed in previous work for LAAS [1-3], it is quite a challenge for the shipboard landing system because of the

differences in the navigation systems. Before going into details of how *VPL*s are computed, two different approaches of using reference measurements will be presented. The first is referred to as the averaging approach, where individual estimates between airborne receiver and each reference receiver are combined in the position domain by weighted average. The other approach, which is referred to as the coupled estimation approach, combines the measurements in the range domain and then estimates the relative position vector.

III. AVERAGING APPROACH

In the averaging method, each airborne-shipboard receiver pair is processed individually and the relative position vector for each pair is estimated. The lever arms between antennas onboard the ship are converted to baseline vectors in the navigation frame using ship attitude information. (In this work, attitude and lever arm survey errors are assumed to be negligible.) Knowing the baseline vectors between the antennas, all estimated vectors can be translated to one reference relative vector.

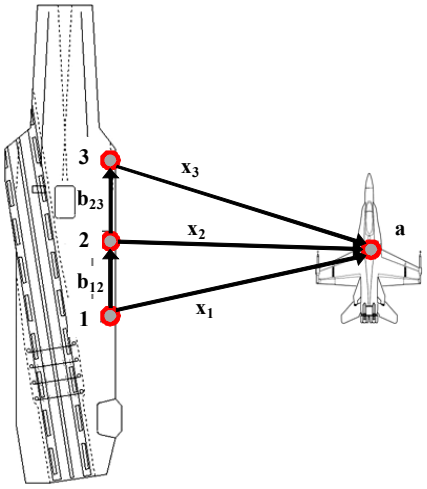

Figure 1: Schematic Diagram for a Ship Equipped with Multi Antennas/Receivers and an Aircraft with a Single Airborne Antenna/Receiver.

For example, if three antennas/receivers are used on the ship, as seen in Figure 1, three individual relative vectors can be estimated $\hat{\mathbf{x}}_1$, $\hat{\mathbf{x}}_2$ and $\hat{\mathbf{x}}_3$. If $\hat{\mathbf{x}}_2$ is used as the reference vector, then the estimates $\hat{\mathbf{x}}_1$ and $\hat{\mathbf{x}}_3$ can be transferred with respect to antenna 2 as:

$$\hat{\mathbf{x}}_2^{(1)} = \hat{\mathbf{x}}_1 - \mathbf{b}_{12} \tag{9}$$

$$\hat{\mathbf{x}}_2^{(2)} = \hat{\mathbf{x}}_2 \tag{10}$$

$$\hat{\mathbf{x}}_2^{(3)} = \hat{\mathbf{x}}_3 + \mathbf{b}_{23} \tag{11}$$

Under the H0 hypothesis, where all three antennas are assumed fault free, these three vectors can be averaged to produce one vector $\hat{\mathbf{x}}_0$. However, averaging, must account for the quality of the individual estimates. Therefore, a weighted average is performed. The averaged $\hat{\mathbf{x}}_0$ can be estimated by solving the following model,

$$\begin{bmatrix} \hat{\mathbf{x}}_2^{(1)} \\ \hat{\mathbf{x}}_2^{(2)} \\ \hat{\mathbf{x}}_2^{(3)} \end{bmatrix} = \begin{bmatrix} \mathbf{I} \\ \mathbf{I} \\ \mathbf{I} \end{bmatrix} \mathbf{x}_0 + \begin{bmatrix} \delta\mathbf{x}_1 \\ \delta\mathbf{x}_2 \\ \delta\mathbf{x}_3 \end{bmatrix} \Rightarrow \mathbf{z}_0 = \mathbf{H}_0\mathbf{x}_0 + \mathbf{v}_0 \tag{12}$$

With the covariance matrix $\mathbf{P}_{xn\,xm}$ defined as $E\{\delta\mathbf{x}_n\,\delta\mathbf{x}_m^T\}$, the covariance of the error $\mathbf{v}_0$ is written as (assuming perfect knowledge of $\mathbf{b}_{12}$ and $\mathbf{b}_{23}$),

$$\mathbf{R}_0 = \begin{bmatrix} \mathbf{P}_{x1x1} & \mathbf{P}_{x1x2} & \mathbf{P}_{x1x3} \\ \mathbf{P}_{x1x2}^T & \mathbf{P}_{x2x2} & \mathbf{P}_{x2x3} \\ \mathbf{P}_{x1x3}^T & \mathbf{P}_{x2x3}^T & \mathbf{P}_{x3x3} \end{bmatrix} \tag{13}$$

For example, the covariance of the estimate error in $\hat{\mathbf{x}}_2^{(n)}$ is $E\{(\hat{\mathbf{x}}_2 - \mathbf{x}_2)(\hat{\mathbf{x}}_2 - \mathbf{x}_2)^T\} = E\{\delta\mathbf{x}_2\,\delta\mathbf{x}_2^T\} = \mathbf{P}_{x2x2}$.

Since the aircraft measurement is common to all three baselines and is used in estimating the three position estimates $\hat{\mathbf{x}}_1$, $\hat{\mathbf{x}}_2$ and $\hat{\mathbf{x}}_3$, the off diagonal blocks of $\mathbf{R}_0$ ($\mathbf{P}_{x1x2}$, $\mathbf{P}_{x1x3}$ and $\mathbf{P}_{x2x3}$) are not zero and must be evaluated. In LAAS, the off diagonal terms could easily be expressed in terms of raw measurement noise standard deviations because the position estimation in LAAS is based on a least squares method. In the shipboard landing navigation algorithm, however, Kalman filters are used to estimate the individual relative vectors. Therefore, it is quite challenging to write the off diagonal block matrices in $\mathbf{R}_0$ in terms of the raw measurement noise variance. A new method to account for correlated KF estimates must be derived.

Correlated KF's

In this subsection, the cross covariance of two correlated state vectors that were each estimated using Kalman filters is derived. To be general, no assumption is made in this derivation about what kind of states these vectors include. These two estimated vectors will be referred to as $\hat{\mathbf{x}}_1$ and $\hat{\mathbf{x}}_2$. The measurement update will be discussed first. In order to estimate $\mathbf{x}_1$ and $\mathbf{x}_2$ at time *k*, the Kalman filter equations 14 and 15 are used, respectively [6]. (Notice that the time subscript *k* is removed from the equations for clarity.)

$$\hat{\mathbf{x}}_1 = \bar{\mathbf{x}}_1 + \mathbf{K}_1(\mathbf{z}_1 - \mathbf{H}_1\bar{\mathbf{x}}_1) \tag{14}$$

$$\hat{\mathbf{x}}_2 = \bar{\mathbf{x}}_2 + \mathbf{K}_2(\mathbf{z}_2 - \mathbf{H}_2\bar{\mathbf{x}}_2) \tag{15}$$

where,

$\bar{\mathbf{x}}_1$ and $\bar{\mathbf{x}}_2$: *a priori* estimates of $\mathbf{x}_1$ and $\mathbf{x}_2$
$\mathbf{K}_1$ and $\mathbf{K}_2$: Kalman gains for $\mathbf{x}_1$ and $\mathbf{x}_2$
$\mathbf{z}_1$ and $\mathbf{z}_2$: measurements from receivers 1 and 2
$\mathbf{H}_1$ and $\mathbf{H}_2$: the observation matrices for $\mathbf{x}_1$ and $\mathbf{x}_2$

Therefore, by definition, the cross covariance matrix ($\hat{\mathbf{P}}_{x1x2}$) between the error in the estimates $\hat{\mathbf{x}}_1$ and $\hat{\mathbf{x}}_2$ is,

$$\hat{\mathbf{P}}_{x1x2} = E\left\{\left(\mathbf{x}_1 - \hat{\mathbf{x}}_1\right)\left(\mathbf{x}_2 - \hat{\mathbf{x}}_2\right)^T\right\} \tag{16}$$

Substituting Equations 14 and 15 in 16, $\hat{\mathbf{P}}_{x1x2}$ becomes,

$$\begin{aligned}\hat{\mathbf{P}}_{x1x2} = \\ E\{&\left[\left(\mathbf{I} - \mathbf{K}_1\mathbf{H}_1\right)\left(\mathbf{x}_1 - \bar{\mathbf{x}}_1\right) - \mathbf{K}_1\mathbf{v}_1\right] \\ &\left[\left(\mathbf{I} - \mathbf{K}_2\mathbf{H}_2\right)\left(\mathbf{x}_2 - \bar{\mathbf{x}}_2\right) - \mathbf{K}_2\mathbf{v}_2\right]^T\}\end{aligned} \tag{17}$$

where $\mathbf{v}_1$ and $\mathbf{v}_2$ are the measurement noise vectors for $\mathbf{z}_1$ and $\mathbf{z}_2$, respectively. Assuming that the prior estimates and the current measurement noises are independent, Equation 17 can be simplified to,

$$\begin{aligned}\hat{\mathbf{P}}_{x1x2} = \\ &\left(\mathbf{I} - \mathbf{K}_1\mathbf{H}_1\right)E\left\{\left(\mathbf{x}_1 - \bar{\mathbf{x}}_1\right)\left(\mathbf{x}_2 - \bar{\mathbf{x}}_2\right)^T\right\}\left(\mathbf{I} - \mathbf{K}_2\mathbf{H}_2\right)^T \\ &+ \mathbf{K}_1 E\left\{\mathbf{v}_1\,\mathbf{v}_2^T\right\}\mathbf{K}_2^T\end{aligned} \tag{18}$$

The expected value in the first term in the right hand side will be referred to as $\bar{\mathbf{P}}_{x1x2}$ and will be discussed shortly in the time propagation of the Kalman filter. The expected value in the second term is where the correlation between these two estimates, caused by correlated measurements noises due to the common air receiver, can be captured. This term will be referred to as $\mathbf{V}_{12}$ and is basically the cross correlation between the measurement noises from the two tracks. Therefore, the resulting expression for the covariance at time *k* is:

$$\begin{aligned}\hat{\mathbf{P}}_{x1x2,k} = &\left(\mathbf{I} - \mathbf{K}_{1,k}\mathbf{H}_{1,k}\right)\bar{\mathbf{P}}_{x1x2,k}\left(\mathbf{I} - \mathbf{K}_{2,k}\mathbf{H}_{2,k}\right)^T \\ &+ \mathbf{K}_{1,k}\mathbf{V}_{12,k}\,\mathbf{K}_{2,k}^T\end{aligned} \tag{19}$$

In Equation 19, $\mathbf{K}_1$, $\mathbf{K}_2$, $\mathbf{H}_1$ and $\mathbf{H}_2$ are all known from the individual Kalman filters that are implemented for each individual track. Detailed discussions of how to evaluate $\mathbf{V}_{12}$ and how to initialize the covariance propagation in Equation 19 are provided in Appendix A and Appendix B, respectively. Notice that in order to be able to use Equation 19 to compute $\hat{\mathbf{P}}_{x1x2}$ the full state vector (position, ambiguities, multipath, etc.) that is used in estimating the position in each individual filter must be used.

In order to derive a formula for $\bar{\mathbf{P}}_{x1x2}$, we start with the time update Kalman filter equations for $\mathbf{x}_1$ and $\mathbf{x}_2$, respectively:

$$\bar{\mathbf{x}}_{1,k} = \mathbf{F}_{1,(k-1)}\hat{\mathbf{x}}_{1,(k-1)} \tag{20}$$

$$\bar{\mathbf{x}}_{2,k} = \mathbf{F}_{2,(k-1)}\hat{\mathbf{x}}_{2,(k-1)} \tag{21}$$

where $\mathbf{F}_1$ and $\mathbf{F}_2$ are the dynamic transition matrices for $\mathbf{x}_1$ and $\mathbf{x}_2$, respectively. By definition, the cross covariance matrix $\bar{\mathbf{P}}_{x1x2,k}$ is:

$$\bar{\mathbf{P}}_{x1x2,k} = E\left\{\left(\mathbf{x}_{1,k} - \bar{\mathbf{x}}_{1,k}\right)\left(\mathbf{x}_{2,k} - \bar{\mathbf{x}}_{2,k}\right)^T\right\} \tag{22}$$

Substituting Equations 20 and 21 in Equation 22:

$$\begin{aligned}\bar{\mathbf{P}}_{x1x2,k} = \\ E\{&\left[\mathbf{F}_{1,(k-1)}\left(\mathbf{x}_{1,(k-1)} - \hat{\mathbf{x}}_{1,(k-1)}\right) + \mathbf{w}_{1,(k-1)}\right] \\ &\left[\mathbf{F}_{2,(k-1)}\left(\mathbf{x}_{2,(k-1)} - \hat{\mathbf{x}}_{2,(k-1)}\right) + \mathbf{w}_{2,(k-1)}\right]^T\}\end{aligned} \tag{23}$$

where $\mathbf{w}_1$ and $\mathbf{w}_2$ are the process noise vectors for states $\mathbf{x}_1$ and $\mathbf{x}_2$, respectively. Assuming that the process noise is independent from the estimates, Equation 23 can be further simplified to:

$$\begin{aligned}\bar{\mathbf{P}}_{x1x2,k} = \\ &\mathbf{F}_{1,(k-1)}E\left\{\left(\mathbf{x}_{1,(k-1)} - \hat{\mathbf{x}}_{1,(k-1)}\right)\left(\mathbf{x}_{2,(k-1)} - \hat{\mathbf{x}}_{2,(k-1)}\right)^T\right\}\mathbf{F}_{2,(k-1)}^T \\ &+ E\left\{\mathbf{w}_{1,(k-1)}\,\mathbf{w}_{2,(k-1)}^T\right\}\end{aligned} \tag{24}$$

From Equation 16, the first expected value in the right hand side of Equation 24 is $\hat{\mathbf{P}}_{x1x2,(k-1)}$. The second expected value in Equation 24 is the cross covariance of the process noise between the two tracks, which will be referred to as $\mathbf{Q}_{12,(k-1)}$. Therefore, the Kalman filter time update (Equation 24) can be rewritten as,

$$\bar{\mathbf{P}}_{x1x2,k} = \mathbf{F}_{1,(k-1)}\,\hat{\mathbf{P}}_{x1x2,(k-1)}\mathbf{F}_{2,(k-1)}^T + \mathbf{Q}_{12,(k-1)} \tag{25}$$

In Equation 25, the dynamic matrices $\mathbf{F}_1$ and $\mathbf{F}_2$ are known and already evaluated from the individual Kalman filter time updates. The evaluation of the cross covariance process noise $\mathbf{Q}_{12}$ is discussed in Appendix C.

As a result, Equations 19 and 25 can be used to evaluate the off diagonal block matrices of $\mathbf{R}_0$ in Equation 13. Remember, however, that Equations 19 and 25 provide the covariance of the state vector (including all states, not only position) and that only the position covariance is used in $\mathbf{R}_0$. Therefore, only the 3×3 sub-

matrix corresponding to the position states is extracted from $\hat{\mathbf{P}}_{x1x2,k}$ and used in $\mathbf{R}_0$.

Using the weighted least squares estimation method, $\hat{\mathbf{x}}_0$ and its covariance can be written as,

$$\hat{\mathbf{x}}_0 = \left(\mathbf{H}_0^T \mathbf{R}_0^{-1} \mathbf{H}_0\right)^{-1} \mathbf{H}_0^T \mathbf{R}_0^{-1} \mathbf{z}_0 \tag{26}$$

$$\mathbf{P}_{\mathbf{x}0} = \left(\mathbf{H}_0^T \mathbf{R}_0^{-1} \mathbf{H}_0\right)^{-1} \tag{27}$$

$\sigma_{v|H0}$ in Equation 6 that is used to evaluate VPL_{H0} can be computed from the (3,3) element of $\mathbf{P}_{\mathrm{x}0}$ as $\sigma_{v|H0} = \sqrt{\mathbf{P}_{\mathbf{x}0(3,3)}}$.

Now that the H0 hypothesis calculation is done for the averaging method, attention is directed toward the H1*j* hypothesis. Remember that under the H1*j* hypothesis, the j^{th} receiver will be considered faulty and unavailable. For example, for j=1, receivers 2 and 3 are used to estimate an average estimate of the relative vector (referred to as $\hat{\mathbf{x}}_{11}$). Similar to Equation 12, this can be modeled as,

$$\begin{bmatrix} \hat{\mathbf{x}}_2^{(2)} \\ \hat{\mathbf{x}}_2^{(3)} \end{bmatrix} = \begin{bmatrix} \mathbf{I} \\ \mathbf{I} \end{bmatrix} \mathbf{x}_{11} + \begin{bmatrix} \delta \mathbf{x}_2 \\ \delta \mathbf{x}_3 \end{bmatrix} \Rightarrow \mathbf{z}_{11} = \mathbf{H}_{11} \mathbf{x}_{11} + \mathbf{v}_{11} \tag{28}$$

with a measurement noise ,

$$\mathbf{R}_{11} = \begin{bmatrix} \mathbf{P}_{x2x2} & \mathbf{P}_{x2x3} \\ \mathbf{P}_{x2x3}^T & \mathbf{P}_{x3x3} \end{bmatrix} \tag{29}$$

All the block matrices in Equation 29 have already been evaluated in computing $\hat{\mathbf{x}}_0$ earlier. As a result, $\hat{\mathbf{x}}_{11}$ can be estimated as,

$$\hat{\mathbf{x}}_{11} = \left(\mathbf{H}_{11}^T \mathbf{R}_{11}^{-1} \mathbf{H}_{11}\right)^{-1} \mathbf{H}_{11}^T \mathbf{R}_{11}^{-1} \mathbf{z}_{11} \tag{30}$$

with a covariance,

$$\mathbf{P}_{\mathbf{x}11} = \left(\mathbf{H}_{11}^T \mathbf{R}_{11}^{-1} \mathbf{H}_{11}\right)^{-1} \tag{31}$$

The 3rd element of the vectors $\hat{\mathbf{x}}_0$ and $\hat{\mathbf{x}}_{11}$ are extracted and used to compute $|v_0 - v_{11}|$ while the (3,3) element of $\mathbf{P}_{\mathrm{x}11}$ is extracted to compute $\sigma_{v|H11}$ as,

$$\sigma_{v|H11} = \sqrt{\mathbf{P}_{\mathbf{x}11(3,3)}} \tag{32}$$

With $|v_0 - v_{11}|$ and $\sigma_{v|H11}$ being evaluated, VPL_{H11} can be computed using Equation 7. A similar procedure can be followed to compute VPL_{H12} and VPL_{H13}.

Now that VPL_{H0} and VPL_{H1j} are evaluated, the only measure that is left is $PVPL_{H1j}$ (Equation 8). Therefore, it is necessary to derive a formula for computing $\sigma_{|v0-v1j|}$. In deriving such a formula, and for simplicity, we will work on an example of estimating $\sigma_{|v0-v11|}$. Remember that in the estimation of $\mathbf{x}_0$ and $\mathbf{x}_{11}$ the same airborne receiver, in addition to reference receivers 2 and 3, are used. Therefore, $\hat{\mathbf{x}}_0$ and $\hat{\mathbf{x}}_{11}$ are correlated. If the cross correlation covariance matrix between these two vectors is referred to as $\mathbf{P}_{\mathrm{x}0\mathrm{x}11}$, then the covariance of $\hat{\mathbf{x}}_0 - \hat{\mathbf{x}}_{11}$ ($\mathbf{P}_{\mathrm{x}0\text{-}\mathrm{x}11}$) can be written in terms of $\mathbf{P}_{\mathrm{x}0}$, $\mathbf{P}_{\mathrm{x}11}$ and $\mathbf{P}_{\mathrm{x}0\mathrm{x}11}$ as,

$$\mathbf{P}_{\mathbf{x}0-\mathbf{x}11} = \mathbf{P}_{\mathbf{x}0} - \mathbf{P}_{\mathbf{x}0\mathbf{x}11} - \mathbf{P}_{\mathbf{x}0\mathbf{x}11}^T + \mathbf{P}_{\mathbf{x}11} \tag{33}$$

Since both $\hat{\mathbf{x}}_0$ and $\hat{\mathbf{x}}_{11}$ are computed using least squares estimation equations (Equations 26 and 30), the estimate errors for $\hat{\mathbf{x}}_0$ and $\hat{\mathbf{x}}_{11}$ can be written as in Equations 34 and 35, respectively.

$$\left(\hat{\mathbf{x}}_0 - \mathbf{x}\right) = \left(\mathbf{H}_0^T \mathbf{R}_0^{-1} \mathbf{H}_0\right)^{-1} \mathbf{H}_0^T \mathbf{R}_0^{-1} \mathbf{v}_0 \tag{34}$$

$$\left(\hat{\mathbf{x}}_{11} - \mathbf{x}\right) = \left(\mathbf{H}_{11}^T \mathbf{R}_{11}^{-1} \mathbf{H}_{11}\right)^{-1} \mathbf{H}_{11}^T \mathbf{R}_{11}^{-1} \mathbf{v}_{11} \tag{35}$$

Therefore, by definition, $\mathbf{P}_{\mathrm{x}0\mathrm{x}11}$ is written as,

$$\begin{aligned} \mathbf{P}_{x0x11} &= E\left\{\left(\hat{\mathbf{x}}_0 - \mathbf{x}\right)\left(\hat{\mathbf{x}}_{11} - \mathbf{x}\right)^T\right\} \\ &= \left(\mathbf{H}_0^T \mathbf{R}_0^{-1} \mathbf{H}_0\right)^{-1} \mathbf{H}_0^T \mathbf{R}_0^{-1} \mathbf{R}_{0,11} \mathbf{R}_{11}^{-1} \mathbf{H}_{11} \left(\mathbf{H}_{11}^T \mathbf{R}_{11}^{-1} \mathbf{H}_{11}\right)^{-1} \end{aligned} \tag{36}$$

where $\mathbf{R}_{0,11} = E\left\{\mathbf{v}_0 \mathbf{v}_{11}^T\right\}$. Since the correlation between the individual estimates have already been evaluated, $\mathbf{R}_{0,11}$ (non-square covariance matrix) can be easily extracted from $\mathbf{R}_0$. In this case for example, the expression for $\mathbf{R}_{0,11}$ becomes,

$$\mathbf{R}_{0,11} = E\left\{\begin{bmatrix} \delta\mathbf{x}_1 \\ \delta\mathbf{x}_2 \\ \delta\mathbf{x}_3 \end{bmatrix} \begin{bmatrix} \delta\mathbf{x}_2 & \delta\mathbf{x}_3 \end{bmatrix}\right\} = \begin{bmatrix} \mathbf{P}_{\mathbf{x}1\mathbf{x}2} & \mathbf{P}_{\mathbf{x}1\mathbf{x}3} \\ \mathbf{P}_{\mathbf{x}2\mathbf{x}2} & \mathbf{P}_{\mathbf{x}2\mathbf{x}3} \\ \mathbf{P}_{\mathbf{x}3\mathbf{x}2} & \mathbf{P}_{\mathbf{x}3\mathbf{x}3} \end{bmatrix} \tag{37}$$

Comparing the result in Equation 37 with the expression of $\mathbf{R}_0$ in Equation 13, it is noticed that $\mathbf{R}_{0,11}$ is $\mathbf{R}_0$ with the first block-column removed. Notice that the first block-column in this case corresponds to the faulty receiver. As a result, $\mathbf{P}_{\mathrm{x}0\text{-}\mathrm{x}11}$ in Equation 33 can be computed and $\sigma_{|v0-v11|}$ can be evaluated as,

$$\sigma_{|v0-v11|} = \sqrt{\mathbf{P}_{\mathbf{x}0-\mathbf{x}11,(3,3)}} \tag{38}$$

Following a similar procedure to compute $\sigma_{|v0-v1j|}$ for any receiver j, $PVPL_{H1j}$ is computed for all reference receivers using Equation 8.

Since all components of the H1 algorithm (VPL_{H0}, VPL_{H1j} and $PVPL_{H1j}$) have been evaluated for the averaging method, the following section will discuss deriving similar expressions for the coupled estimation method.

IV. COUPLED ESTIMATION APPROACH

In the coupled estimation approach, measurements from different reference receivers are translated to a single reference receiver using the lever arm information and the attitude of the ship. By combining these measurements at one common reference point, a single relative position vector is estimated. The advantage in incorporating the geometry constraint directly prior to fixing the cycle ambiguities is that cycle ambiguity observability is improved. In this work, measurements from different reference receivers are assumed to be independent. For simplicity of the derivation and without the loss of generality, assume that we have only two reference receivers. For each reference-air receiver pair, a simplified version of the double difference (user minus reference and satellite minus master-satellite) carrier phase measurement can be written as,

$$\nabla\Delta\boldsymbol{\varphi}_1 = \Delta\mathbf{e}^T\mathbf{x}_1 + \lambda\nabla\Delta\mathbf{N}_1 + \boldsymbol{\varepsilon}_{\Delta\phi 1} \tag{39}$$

$$\nabla\Delta\boldsymbol{\varphi}_2 = \Delta\mathbf{e}^T\mathbf{x}_2 + \lambda\nabla\Delta\mathbf{N}_2 + \boldsymbol{\varepsilon}_{\Delta\phi 2} \tag{40}$$

where,

- $\nabla\Delta\boldsymbol{\varphi}_1$, $\nabla\Delta\boldsymbol{\varphi}_2$: the double difference carrier phase measurement vectors for tracks 1 and 2
- $\Delta\mathbf{e}$: matrix of stacked line of sight vectors
- λ : carrier phase wavelength
- $\nabla\Delta\mathbf{N}_1$, $\nabla\Delta\mathbf{N}_2$: double difference ambiguity vectors for tracks 1 and 2
- $\boldsymbol{\varepsilon}_{\Delta\phi 1}$, $\boldsymbol{\varepsilon}_{\Delta\phi 2}$: the double difference carrier phase measurement noise vectors for tracks 1 and 2

But from Figure 1, $\mathbf{x}_2$ can be written in terms of $\mathbf{x}_1$ as,

$$\mathbf{x}_2 = \mathbf{x}_1 - \mathbf{b}_{12} \tag{41}$$

Using Equation (41) in Equation (40), reordering and writing Equations 39 and 49 in a matrix form results in,

$$\begin{bmatrix} \nabla\Delta\boldsymbol{\varphi}_1 \\ \nabla\Delta\boldsymbol{\varphi}_2 + \Delta\mathbf{e}^T\mathbf{b}_{12} \end{bmatrix} = \begin{bmatrix} \Delta\mathbf{e}^T & \lambda\mathbf{I} & \mathbf{0} \\ \Delta\mathbf{e}^T & \mathbf{0} & \lambda\mathbf{I} \end{bmatrix} \begin{bmatrix} \mathbf{x}_1 \\ \nabla\Delta\mathbf{N}_1 \\ \nabla\Delta\mathbf{N}_2 \end{bmatrix} + \begin{bmatrix} \boldsymbol{\varepsilon}_{\Delta\phi 1} \\ \boldsymbol{\varepsilon}_{\Delta\phi 1} \end{bmatrix} \tag{42}$$

Because the same airborne receiver is used, the double difference carrier phase measurement noise vectors $\boldsymbol{\varepsilon}_{\Delta\phi 1}$ and $\boldsymbol{\varepsilon}_{\Delta\phi 2}$ are correlated. The associated measurement noise matrix accounting for this correlation is derived in Appendix A. As a result, $\mathbf{x}_1$ can be estimated using a Kalman filter. Going back to the multiple-receiver case: in a fault free mode (H0), with all receivers being operational, measurements from all receivers are processed in a similar form as in Equation 42 and $\hat{\mathbf{x}}_0$ and $\mathbf{P}_{x0}$ are estimated using a single Kalman filter. For the H1j case, measurements from all receivers except the j^{th} receiver are used in a similar fashion to estimate $\hat{\mathbf{x}}_{1j}$ and $\mathbf{P}_{x1j}$.

Having $\hat{\mathbf{x}}_0$, $\hat{\mathbf{x}}_{1j}$, $\mathbf{P}_{x0}$ and $\mathbf{P}_{x1j}$, VPL_{H0} and VPL_{H1j} can be computed as explained in the averaging section. As discussed before, the computation of $PVPL_{H1j}$ requires evaluating $\sigma_{|v0-v11|}$. Equations 33 and 38 can be used to evaluate $\sigma_{|v0-v11|}$. The difference between the averaging and coupled approach is in computing $\mathbf{P}_{x0x1j}$. In Equation 36, a formula for computing $\mathbf{P}_{x0x1j}$ was derived based on the fact that $\hat{\mathbf{x}}_0$ and $\hat{\mathbf{x}}_{1j}$ are estimated using least squares estimation. In the coupled estimation approach, both $\hat{\mathbf{x}}_0$ and $\hat{\mathbf{x}}_{1j}$ are estimated using Kalman filters with the same airborne receiver and some common receivers (all except for the j^{th} receiver). A methodology to estimate the cross covariance of two correlated Kalman filter estimates has been developed in the previous section. Therefore, Equations 19 and 25 can be used again to estimate $\mathbf{P}_{x0x1j}$.

Sections II, III and IV (and the appendices) provide a detailed derivation of the H1 algorithm for the two different approaches toward using redundant reference receiver measurements. In order to investigate the advantages and disadvantages of each approach more thoroughly, an availability analysis for the shipboard aircraft landing application is now conducted.

V. AVAILABILITY ANALYSIS

In this section, the performance of the shipboard landing navigation system under the H0 and H1 hypotheses is quantified through availability analysis. The navigation architecture that was defined in Section II and detailed in [4, 5, 9] is used as a basis to determine the covariance of the position estimate error. This covariance is then used to compute $\sigma_{v|H0}$, $\sigma_{v|H1j}$ and $\sigma_{|v0-v1j|}$ for both the averaging and coupled estimation approaches as discussed in Sections III and IV. Next, *VPL*, which will be compared to *VAL*, can be evaluated based on the values and relations in Section II. In order to account for the GPS satellite geometry change, availability analysis is

performed by simulating 1440 satellite geometries (one geometry per minute during the day). Availability is then calculated as the percentage of cases (geometries) for which *VPL* is less than *VAL*.

H0 and H1 availability for the averaging approach is compared to the coupled estimation approach for two scenarios depending on the number of reference receivers that are installed in the ship: two reference receivers and three reference receivers. In addition, availability in the case where the ship is equipped with a single reference receiver is evaluated as a baseline for comparison. In these scenarios, a single airborne receiver is assumed. The requirements and simulation parameters that are used in evaluating the availability are not necessarily the requirements that are used currently in the shipboard landing navigation system. Nevertheless, example requirements that are chosen based on those given in [8], [9] and [13] are used (Table 1). In this simulation, the standard deviation of the carrier phase (single difference) measurement noise $\sigma_{\Delta\phi}$ and single difference pseudorange code $\sigma_{\Delta PR}$ are assumed to be 1 cm and 50 cm, respectively. The single difference standard deviations $\sigma_{\Delta PR}$ and $\sigma_{\Delta\phi}$ are related to the raw values (σ_{PR} and σ_{ϕ}) by a scaling factor of $\sqrt{2}$. In this analysis, a maximum airborne prefiltering period of 5 minutes is used to generate floating estimates of the widelane cycle ambiguities. In other words, if the satellite has been visible by the aircraft for a period of time longer than the maximum prefiltering time, the prefiltering time is set to the maximum prefiltering time. It is assumed that the ship has been running the filter for a long time (the maximum prefiltering time is set to the time since the satellite first came in view). The remaining simulation parameters are summarized in Table 1.

Table 1: Simulation Parameters

Parameter	Value
$P_v(MI\|H0)$	10^{-7}
P(H1)	10^{-5}
Continuity risk req.	10^{-6}
VAL	1.8 m
PIF threshold	10^{-8}
Satellite constellation	Almanac of May 15 2007
Location	Atlantic Ocean (27^oN and 74^oW)
Maximum prefiltering time	5 minutes
Ship multipath time constant	1 minute
Aircraft multipath Gauss Markov time constant	20 seconds

Using the parameters detailed in Table 1, a covariance analysis simulation is performed and availability is calculated. Table 2 shows the availability results for both methods using different numbers of reference receivers. For the H0 case, the averaged method outperforms the single reference receiver case by 9% (for two receivers) to 18% (three receivers). The performance of the coupled estimation method, on the other hand, is superior compared to the averaging method (availability gain is approximately 19% for two antennas and 15% for three antennas). This gain in availability is attributed to cycle resolution enhancement in the coupled estimation method. Based on Section III and IV, the implementation of the H0 algorithm in the averaged estimation method is more complicated than that in the coupled estimation method. In the coupled estimation, a single Kalman filter (KF) for the fused measurements from different antennas is used to estimate the relative position vector. In the averaging method with two antennas for example, two Kalman filters are required to estimate the two individual vectors with a third Kalman filter to estimate the correlation between the two individual estimates due to common airborne receiver. Furthermore, a least squares (LS) estimation process is used to average the two individual estimates.

Table 2: Availability Results

		H0 Availability	H1 Availability
	1 Rcvr.	65.0 %	0 %
Averaged	2 Rcvr.	74.5 %	74.5 %
	3 Rcvr.	83.2 %	83.2 %
Coupled	2 Rcvr.	95.4 %	93.7 %
	3 Rcvr.	97.9 %	97.9 %

The performance of this navigation algorithm is also evaluated under the H1 hypothesis. For a single reference receiver, the availability is zero regardless of the integrity requirement because the continuity requirement cannot be fulfilled. In the multi receiver case, the results in Table 2 show that the H1 hypothesis has little impact on availability compared to H0. This is explained by the fact that the accuracy requirement is more stringent than the integrity requirement, and the integrity isn't limiting availability. Since H1 hypothesis affects integrity and not accuracy, availability was not greatly affected. Therefore, the coupled estimation provides the optimal performance in terms of availability, accuracy and integrity compared to single receiver and to the averaging method that was used in LAAS.

Unfortunately, the performance enhancement using the coupled estimation method comes with a cost. Table 3 shows the number of states and measurements (assuming 12 visible satellites with L1/L2 measurements) that are required for the cases in Table 2. These numbers have an impact on the computation time and memory allocation for each of these algorithms, which can be crucial for real time implementation. Remember that an inversion of a matrix with size equal to the measurement vectors is necessary in the Kalman filter. Also, matrix sizes are

based on both the number of measurements and the number of states. For example, although the coupled estimation under the H0 hypothesis provides the best performance for three antennas, the coupled Kalman filter is composed of 66 double difference L1/L2 carrier phase measurements and 135 states: 3 states for position, 66 states for double difference L1/L2 ambiguities and 66 for double difference multipath states. On the other hand, each of the six individual Kalman filters in the averaging method has only 22 measurements and 45 states. Although, extra least squares estimation computations are necessary in the averaging method, the size of the least squares estimation for three antennas is small (9×9) compared to the Kalman filter.

Different techniques can be introduced to increase the computation efficiency of coupled estimation by reducing the number of states and reducing the number of measurements per Kalman filter measurement update. These techniques are not discussed in this paper but few examples are mentioned as alternatives in order to enhance the computation efficiency. Examples of these techniques include the UD Kalman filter [16] and the measurement differencing Kalman filter [14, 15]. Another alternative is to perform the measurement updates for uncorrelated measurements separately in the Kalman filter, which reduces the size of the computation load in the matrix inversion. For example, L1 and L2 measurement updates can be performed individually because the L1 and L2 measurement errors are uncorrelated. Currently, a real time implementation of these algorithms is underway. Therefore, in the future, a real time timing analysis will be added to Table 3 and, if any, the computation enhancement techniques that were used.

Table 3: Number of Kalman filters and least squares including number of measurements and states required for implementation.

		Averaged		Coupled	
		2 Rcvr.	3 Rcvr.	2 Rcvr.	3 Rcvr.
H0	No. of KF	3	6	1	1
	States/Meas.	47/22	47/22	91/44	135/66
	No. of LS/states	1/6	1/9	0	0
H1 (only)	No. of KF	0	0	4	6
	States/Meas.	0	0	47/22	91/44
	No. of LS/states	2/6	6/9	0	0

CONCLUSIONS

A methodology to mitigate single receiver failures for carrier phase navigation architectures was developed. In addition, two different approaches to utilize redundant carrier phase measurements from multiple reference receivers were described: averaging approach and coupled estimation approach. The impact of using these different methods on accuracy and integrity were investigated. The navigation performance, measured by availability under both the fault free and single receiver failure hypotheses, was superior for the coupled estimation as compared to the averaging method. Different perspectives such as implementation complexity and computational efficiency have also been discussed for both approaches. Although the coupled estimation is relatively easier to implement than the averaging method, it might require more computational power.

APPENDIX A: COVARIANCE OF THE CORRELATED MEASUREMENT NOISE $\mathbf{V}_{12}$

$\mathbf{V}_{12}$ is defined in Equations 18 and 19 as the cross correlation between the two measurement noise vectors $\mathbf{v}_1$ and $\mathbf{v}_2$. However, $\mathbf{v}_1$ and $\mathbf{v}_2$ are simplified notations for the double difference carrier phase measurements for tracks 1 and 2. For example, $\mathbf{v}_1$ can be expanded in terms of the raw carrier phase measurement noise (ε_ϕ) from reference receiver 1, air receiver *a*, satellite *k*, and reference satellite *l* as:

$$v_1 = \varepsilon_{\phi 1}^{k} - \varepsilon_{\phi a}^{k} - \varepsilon_{\phi 1}^{l} + \varepsilon_{\phi a}^{l} \tag{43}$$

In deriving $\mathbf{V}_{12}$, the following assumptions are used:

1- Measurement noises from different reference receivers are independent (uncorrelated).
2- Measurement noises from different satellites are independent (uncorrelated).

The elements of the $\mathbf{V}_{12}$ covariance matrix are composed based on the following:

a. Elements where reference receivers 1 and 2 are using the same satellites *k* and *l*. In this scenario, the element of $\mathbf{V}_{12}$ (noted v_{12}) is:

$$\begin{aligned} v_{12} = & \\ & E\left\{\left(\varepsilon_{\phi 1}^{k} - \varepsilon_{\phi a}^{k} - \varepsilon_{\phi 1}^{l} + \varepsilon_{\phi a}^{l}\right)\right. \\ & \left.\left(\varepsilon_{\phi 2}^{k} - \varepsilon_{\phi a}^{k} - \varepsilon_{\phi 2}^{l} + \varepsilon_{\phi a}^{l}\right)^{T}\right\} \end{aligned} \tag{44}$$

which can be simplified using assumptions 1 and 2 above to,

$$\begin{aligned} v_{12} &= E\left\{\varepsilon_{\phi a}^{k}\ \varepsilon_{\phi a}^{k\ T}\right\} + E\left\{\varepsilon_{\phi a}^{l}\ \varepsilon_{\phi a}^{l\ T}\right\} \\ &= \sigma_{\phi a,k}^{2} + \sigma_{\phi a,l}^{2} \end{aligned} \tag{45}$$

where $\sigma_{\phi a,k}$ and $\sigma_{\phi a,l}$ are the standard deviations of the carrier phase measurement noises for receiver *a* and satellites *k* and *l*, respectively.

Assuming that the same carrier phase measurement noise variance is used for all receivers and satellites, v_{12} in Equation 45 can be further simplified in terms of raw carrier phase measurement noise variance (σ_ϕ^2) or in terms of the single difference one ($\sigma_{\Delta\phi}^2$) to,

$$v_{12} = 2\sigma_\phi^2 = \sigma_{\Delta\phi}^2 \tag{46}$$

b. Elements where reference receivers 1 and 2 are using different satellites but the same reference satellite *l*. Following the same steps in the derivation (Equations 44 to 46) as in case-a, v_{12} in this case is,

$$v_{12} = E\left\{\varepsilon_{\phi a}^{l}\ \varepsilon_{\phi a}^{l\ T}\right\} = \sigma_{\phi al}^2 \tag{47}$$

or in terms of Equation 46,

$$v_{12} = \sigma_\phi^2 = \frac{\sigma_{\Delta\phi}^2}{2} \tag{48}$$

c. Elements where reference receivers 1 and 2 are using the same satellite *k* but different reference satellites. Following the same steps in a and b above, v_{12} in this case is,

$$v_{12} = E\left\{\varepsilon_{\phi a}^{k}\ \varepsilon_{\phi a}^{k\ T}\right\} = \sigma_{\phi ak}^2 \tag{49}$$

or in terms of Equation 45,

$$v_{12} = \sigma_\phi^2 = \frac{\sigma_{\Delta\phi}^2}{2} \tag{50}$$

d. Elements where reference receivers 1 and 2 are using different satellites and different reference satellites as well. Following the same steps in the derivation of cases a to c above, v_{12} in this case is zero.

$$v_{12} = 0 \tag{51}$$

APPENDIX B: INITIAL $\overline{\mathbf{P}}_{x1x2,0}$

The initial covariance $\overline{\mathbf{P}}_{x1x2,0}$ is the covariance of the initial estimates between states $\mathbf{x}_1$ and $\mathbf{x}_2$, where $\mathbf{x}_1$ and $\mathbf{x}_2$ might not only be the position states, but all estimated states as mentioned in Section III. From Equation 19, $\overline{\mathbf{P}}_{x1x2,0}$ is defined as $\overline{\mathbf{P}}_{x1x2,0} = E\left\{\left(\mathbf{x}_{1,0} - \overline{\mathbf{x}}_{1,0}\right)\left(\mathbf{x}_{2,0} - \overline{\mathbf{x}}_{2,0}\right)^T\right\}$. Therefore, the initial $\overline{\mathbf{P}}_{x1x2,0}$ depends on the type of state that is initialized and the value it is initialized within the Kalman filter. The following are some examples of estimated states that are frequently used in GPS algorithms with their corresponding initial $\overline{\mathbf{P}}_{x1x2,0}$:

- Position states: Remember that the true position states are the same for both tracks (by definition). Therefore, if the two tracks are initiated similarly, say with zero value and a covariance **P**, then the elements of $\overline{\mathbf{P}}_{x1x2,0}$ corresponding to the position states will also be **P**.

- Ambiguity states: the true ambiguities are generally different for different receivers. However, the elements of $\overline{\mathbf{P}}_{x1x2,0}$ corresponding to the ambiguity states depend on how the ambiguities are initialized in the individual filters. For example, if they are initialized with zero values and infinitely large covariance, then the covariance of the ambiguities in $\overline{\mathbf{P}}_{x1x2,0}$ is zero. If the ambiguities are initialized with the carrier minus code measurements and the code covariance, then the ambiguity elements of $\overline{\mathbf{P}}_{x1x2,0}$ are the associated covariance of the measurement noise between the individual tracks. This covariance matrix can be built following similar procedure to the one in Appendix A but for code measurement noise instead of the carrier noise.

- Multipath states: the multipath colored error is usually modeled as first order Gauss Markov process. The single difference multipath state from the two tracks are therefore correlated due to the existence of the same air antenna. Therefore, the initial $\overline{\mathbf{P}}_{x1x2,0}$ for the multipath states is correlated in a similar fashion as the measurements.

- Atmospheric model states (ionospheric gradient and tropospheric refractivity index states): the true states in these cases are identical for both tracks (the air antenna and the reference antennas are usually within a short distance where atmospheric errors are totally correlated). Therefore, if these states are initialized with the same values in both tracks, (which is the case, and they are usually initialized with a value of zero), then $\overline{\mathbf{P}}_{x1x2,0}$ for these states is totally correlated for the same satellites (the covariance elements will be identical to the ones for each individual track).

APPENDIX C: COVARIANCE OF THE CORRELATED PROCESS NOISE $\mathbf{Q}_{12}$

The cross covariance process noise $\mathbf{Q}_{12}$ in Equation 25 is defined as the covariance between process noises on the states for tracks 1 and 2. Therefore, the terms in $\mathbf{Q}_{12}$ will depend on the type of the process noise in each state. The following are examples of states used frequently in different GPS navigation applications:

- Position states: the true relative position for both tracks is the same. Therefore, the process noise on both tracks is the same as well., and the process noise for the position states is totally correlated (the covariance elements in $\mathbf{Q}_{12}$ is identical to the individual process noise ones).

- Multipath states: the covariance of the process noise for the multipath states depends on the multipath model used. For example, if a first order Gauss Markov model is used, then it is related to the multipath error standard deviation. The value of this standard deviation for the two tracks is correlated due to using the same air receiver (same air multipath). Therefore, the correlated process noise covariance can be evaluated in a similar fashion to the measurement noise $\mathbf{V}_{12}$ in Appendix A.

- Cycle ambiguity and atmospheric states: the covariance of the process noise in these states in the individual tracks is zero. Therefore, the elements of $\mathbf{Q}_{12}$ corresponding to these states is also zero.

ACKNOWLEDGMENT

The authors gratefully acknowledge the Naval Air Systems Command (NAVAIR) of the US Navy for supporting this research. The authors would like to specifically acknowledge the support and guidance of Glenn Colby and Marie Lage regarding this work.

REFERENCES

[1] "Minimum Aviation System Performance Standards for the Local Area Augmentation System Airborne Equipment," *RTCA Document Number DO-245A,* December 2004.

[2] B. Pervan, S. Pullen, and J. Christie, "A Multiple Hypothesis Approach to Satellite Navigation Integrity," *NAVIGATION: Journal of Institute of Navigation,* vol. 45, No. 1, Spring 1998.

[3] F. Liu, T. Murphy, and T. Skidmore, "LAAS Signal-in-Space Integrity Monitoring Description and Verification Plan," in *Proceedings of the 10th International Technical Meeting of the Satellite Division of the Institute of Navigation ION GPS 1997*, Kansas City, MO, Sept. 1997.

[4] S. Khanafseh, "GPS Navigation Algorithms for Autonomous Airborne Refueling of Unmanned Air Vehicles " PhD Thesis, Illinois Institute of Technology, Chicago, IL, May 2008.

[5] S. Langel, S. Khanafseh, F. C. Chan, and B. Pervan, "Cycle Ambiguity Reacquisition in UAV Applications Using a Novel GPS/INS Integration Algorithm " in *Proceedings of the International Technical Meeting of the Satellite Division of the Institute of Navigation ION-ITM 2009*, Anaheim, CA, Jan. 2009.

[6] J. Crassidis and J. Junkins, *Optimal Estimation of Dynamic Systems*. New York, NY: Capman & Hall/CRC, 2004.

[7] P. Misra and P. Enge, *Global Positioning System signals, Measurements, and Performance*. Lincoln, MA: Ganga-Jumuna Press, 2001.

[8] M. Heo, B. Pervan, S. Pullen, J. Gautier, P. Enge, and D. Gebre-Eziabher, "Robust Airborne Navigation Algorithm for SRGPS," in *Proceeding of the IEEE position, Location, and Navigation symposium (PLANS '2004)*, Monterey, CA, Apr. 2004.

[9] M. B. Heo, "Robust Carrier Phase DGPS Navigation for Shipboard Landing of Aircraft." PhD Thesis, Illinois Institute of Technology, Chicago, IL, Dec. 2004.

[10] G. A. McGraw and R. S. Y. Young, "Dual Frequency Smoothing DGPS Performance Evaluation Studies," in *Proceedings of the Institute of Navigation 2005 national Technical Meeting*, San Diego, CA, Jan. 2005.

[11] S. Dogra, J. Wright, and J. Hansen, "Sea-Based JPALS Relative Navigation algorithm Development," in *Proceedings of the Institute of Navigation 2005 GNSS Meeting*, Long Beach, CA, Sept. 2005.

[12] P. Teunissen, "GNSS ambiguity bootstrapping: Theory and Application," in *Proc. KIS2001, International Symposium on Kinematic Systems in Geodesy, Geomatics and Navigation*, Bnaff, Canada.

[13] S. Khanafseh and B. Pervan, "A New Approach for Calculating Position Domain Integrity Risk for Cycle Resolution in Carrier Phase Navigation Systems," in *Proceeding of the IEEE Position, Location, and Navigation Symposium (PLANS '2008)*, Monterey, CA, Apr. 2008.

[14] A. Bryson, *Applied Linear Optimal Control: Examples and Algorithms* New York, NY: Cambridge University Press 2002.

[15] K. O'Keefe, M. Petovello, G. Lachapelle, and M. Cannon, "Assessing Probability of Correct Ambiguity Resolution in the Presence of Time-Correlated Errors," *NAVIGATION: Journal of*

Institute of Navigation, vol. 53, No. 4, Winter 2006.

[16] D. Chiu and K. O'Keefe, "Bierman-Thornton UD Filtering for Double-Differenced Carrier Phase Estimation Accounting for Full Mathematical Correlation," in *Proceedings of the Institute of Navigation 2008 NTM Meeting*, San Diego, CA, Jan. 2008.